

## Article

# An Innovative Waterwheel-Rotating Biological Contactor (WRBC) System for Rural Sewage Treatment

Jiansheng Huang <sup>†</sup>, Xin Wen <sup>\*,†</sup>, Qian Tang, Deshao Liu and Shuangkou Chen

School of Civil Engineering and Architecture, Chongqing University of Science and Technology, Chongqing 400045, China

\* Correspondence: xinwen@cqust.edu.cn

† These authors contributed equally to this work.

**Abstract:** The treatment of rural sewage has become an important part of environmental protection. In this study, a novel waterwheel-rotating biological contactor (WRBC) system, with intensified biofilm and high-shock load resistance, was applied to treat rural sewage. When the COD concentration of actual sewage fluctuated between 79–530 mg/L, the COD removal efficiency was 41.3–94.5%, and the  $\text{NH}_4^+$ -N removal efficiency always reach 100% with actual sewage. The TN removal efficiency changed between 14.3–86.2%, which was greatly affected by the water intake. The effluent TN concentration ranged from 5 to 14 mg/L, which meets the emission requirements. It maintained an absolute effluent stability when the change rates of influent loads (N or COD) varied from –60% to 100%. The biofilm morphology and the composition of extracellular polymeric substances were evaluated based on SEM and FTIR spectra. The results showed that the  $-\text{NH}_2$  group content increased compared with the inoculated sludge, and the biofilm formed more uneven compact clusters after the treatment of actual sewage. Based on 16SrRNA high-throughput sequencing techniques, the bacterial diversity and microbial community structure of the WRBC system over time was revealed. This study may help guide optimization strategies for more effective pollutant removal in rural areas.

**Keywords:** rural sewage; WRBC system; biofilm morphology; EPS composition; microbial community



**Citation:** Huang, J.; Wen, X.; Tang, Q.; Liu, D.; Chen, S. An Innovative Waterwheel-Rotating Biological Contactor (WRBC) System for Rural Sewage Treatment. *Water* **2023**, *15*, 1323. <https://doi.org/10.3390/w15071323>

Academic Editor: Stefano Papirio

Received: 21 February 2023

Revised: 21 March 2023

Accepted: 23 March 2023

Published: 28 March 2023



**Copyright:** © 2023 by the authors. Licensee MDPI, Basel, Switzerland. This article is an open access article distributed under the terms and conditions of the Creative Commons Attribution (CC BY) license (<https://creativecommons.org/licenses/by/4.0/>).

## 1. Introduction

Rural sewage usually contains high organic concentrations, which have strong biodegradability [1,2]. Rural residents are mostly scattered, resulting in a wide range of domestic sewage pollution and a large amount of total emissions [3,4]. The seasonal characteristics of rural sewage production are obvious. The emissions in summer are greater than that in winter. Furthermore, the quantity and quality of rural sewage in different regions are different due to different degrees of economic development, local terrain and climate, and customs of various rural areas in China. The improper treatment of rural sewage not only threatens the local sanitary environment and sources of drinking water, but also seriously endangers the safety of the national or regional groundwater environments [5–7]. Therefore, an efficient and reliable treatment technology for rural sewage, which can adapt to the phenomenon of water quality and quantity changing greatly with time and space, is urgently needed.

Common treatment technologies, such as constructed wetlands [8–10], bio-contact oxidation [11,12], biological filters [13–15], and membrane bioreactors [16,17], are used in rural sewage treatment. Compared with those biological treatment methods, the RBC (rotating biological contactor) has potential advantages such as resistance from shock loads and a stable ecological system [18]. In this study, an innovative waterwheel-rotating biological contactor (WRBC) system was set up. It consisted of a waterwheel-rotating biological contactor system (with rotator fillers). A waterwheel cage with buckets attached to it was added to the system to achieve self-reflow during the process of rotation.

A hacketten filler is a product with a three-dimensional structure and a large surface area. It can be installed directly without fixing, and microbes can easily attach to the surface area [19]. This product was selected to fill the waterwheel cage with a smaller carrier volume, larger total surface area, and larger biomass per unit of volume [20]. The biofilm growing on the filler rarely fell off, which preserved the secondary sedimentation tank. In addition, the rotation of the waterwheel made the carriers self-flipping, allowing them to flow with the cyclonic flow of the mixed liquid; this increased the contact area between the biofilm and wastewater per unit of time and provided sufficient oxygen [21].

A novel WRBC system was proposed, the key of which was a waterwheel-rotating cage module. The rotation of the waterwheel made the carriers self-flipping, allowing them to flow, which improved the quality transfer effect and achieved self-reflow at the same time. The performance and stability of treating rural sewage with this system were studied. Another aim was to investigate biofilm characteristics and the shifts of functional microorganisms in the WRBC system.

## 2. Materials and Methods

### 2.1. WRBC System Set-Up

As shown in the graphical abstract, the WRBC system (made of stainless steel) consisted of an anaerobic pool, a waterwheel-rotating cage module, and a sludge/liquid separation module. The working volume of the reactor was 65 L (anaerobic pool: 17 L; waterwheel-rotating cage module: 40 L; and sludge/liquid separation module: 8 L). The waterwheel-rotating cage was filled with hacketten ( $\Phi 25$  mm), with a filling ratio of 100%. The immersion rate of the cage was 40%. The anaerobic pool was filled with fiber bundle packing, with a filling ratio of 20%. Continuous flow mode was controlled by a peristaltic pump during the operation period.

The operation of the WRBC system can be divided into 4 periods: start-up (phase 1), operation with actual sewage (phase 2), stability test (phase 3), and speed adjustment period (phase 4). In the start-up period, activated sludge from the Jiangjin Sewage Treatment Plant was added to the reactor as the inoculated sludge (0.5 g/L). The rotational speed of the waterwheel-rotating cage was set at 4 r/min, since a lower speed was more conducive to biofilm attachment. Actual rural sewage was fed into the WRBC system in phase 2, and the rotational speed of the waterwheel-rotating cage was adjusted to 6 r/min. During the stability testing period, the change rates of influent loads (N, COD, and flow) varied from  $-60\%$  to  $100\%$ , and system performances were observed. The task of the speed adjustment period was to seek the feasibility of increasing the self-reflux rate to enhance the TN removal by raising the rotation speed.

### 2.2. Preparation of Influent

In the start-up period, artificial simulated sewage was used, which was provided by sodium acetate for the carbon source, ammonia chloride and potassium nitrate for the nitrogen source, and potassium dihydrogen phosphate for the phosphate source. Nitrate nitrogen was added to the influents, since the presence of nitrate was found in the investigation of the local rural sewage quality. The reason for the presence of nitrate might be that there are many individual or small-scale cured meat workshops in the area, and local residents have the habit of composting in small puddles. All the sewage enters the system, which contains nitrate nitrogen. Other compounds added for influents preparation included  $\text{MgSO}_4 \cdot 7\text{H}_2\text{O}$ , 50 mg/L;  $\text{CaCl}_2$ , 30 mg/L;  $\text{ZnSO}_4 \cdot 7\text{H}_2\text{O}$ , 0.43 mg/L;  $\text{CuSO}_4 \cdot 5\text{H}_2\text{O}$ , 0.25 mg/L;  $\text{CoCl}_2 \cdot 6\text{H}_2\text{O}$ , 0.24 mg/L;  $\text{Na}_2\text{MoO}_4 \cdot 2\text{H}_2\text{O}$ , 0.22 mg/L;  $\text{MnCl}_2 \cdot 4\text{H}_2\text{O}$ , 0.99 mg/L;  $\text{NiCl}_2 \cdot 6\text{H}_2\text{O}$ , 0.19 mg/L;  $\text{H}_3\text{BO}_4$ , 0.014 mg/L;  $\text{Na}_2\text{WO}_4 \cdot 2\text{H}_2\text{O}$ , 0.05 mg/L; and  $\text{FeSO}_4$ , 6.25 mg/L.

Actual rural sewage was collected from Lijia Village, Shimen Town, Jiangjin District, Chongqing, China, as the influent of phase 2 (see Table 1). Sampling point 1 was closer to the residential houses (with individual-scale livestock breeding), from which wastewater was used on days 20–35. Sampling point 2 was located at the front end of the village sewage establishment facility (the end of the pipe network), and the collected sewage was used

on days 36–61. The sewage quality collected at day 49 changed greatly compared with the previous day due to the arrival of the rainy season and a pipe network without the diversion of rainwater and sewage.

**Table 1.** Influent of the WRBC system in phases 1–2.

Phase	Time	Influent	Inf. Ammonia	Inf. Nitrate	Inf. TN	Inf. COD
1	Days 1–19	Artificial simulated sewage	23.54 ± 1.95	11.65 ± 1.97	35.21 ± 2.75	298 ± 16
2	Days 20–35	Actual rural sewage from sampling point 1	25.10 ± 1.83	10.75 ± 1.36	35.89 ± 2.42	432 ± 50
2	Days 36–48	Actual rural sewage from sampling point 2	54.45 ± 2.30	2.30 ± 1.47	56.75 ± 1.49	142 ± 26
2	Days 49–61	Actual rural sewage from sampling point 2 (rainy)	23.83 ± 1.70	1.42 ± 1.41	25.23 ± 1.30	91 ± 10

In phases 3 and 4, influents consisted of 20% (vol.) actual rural sewage (collected from the sampling point 2) and 80% (vol.) synthetic water, to make the influent more similar to actual rural sewage. In the system stability tests under nitrogen impact loads (days 62–97), the influent COD concentration was 300 mg/L and the HRT was 24 h. The influent nitrogen concentration/37.5 mg/L was set at 40%, 50%, 67%, 100%, 133%, and 200% (The influent nitrogen concentration was about 15 mg/L, 19 mg/L, 25 mg/L, 38 mg/L, 50 mg/L, and 75 mg/L, respectively). In the system stability tests under COD impact loads (days 98–133), the influent COD/TN (total nitrogen) was set at 20 to ensure that the results were not affected by inadequate carbon sources. The HRT was 24 h and the influent COD concentration/300 mg/L was set at 33%, 66%, 100%, 133%, 166%, and 200%. In the system stability tests under flow impact loads (days 134–166), the HRT/24 h was set at 33%, 66%, 100%, 133%, 166%, and 200%.

### 2.3. Analytical Methods

#### 2.3.1. N and COD Concentration

Influent and effluent water samples were taken to measure COD,  $\text{NH}_4^+$ , and TN concentrations according to standard methods for the examination of water and wastewater [22].

#### 2.3.2. The Total Biofilm Amount Measurements

A total of 5 hacketten fillers were soaked in 20% NaOH at 60 °C for 20 min. Then, the biofilm sludge was completely detached by mechanical agitation, filtered, and dried to a constant weight  $W_1$  (mg). The number of hacketten fillers in the reactor was  $n$ . The total biofilm amount equaled  $0.005n W_1$  (mg/L). Considering the non-uniformity of biofilm growth, the results of this method were not necessarily accurate. However, it was sufficient to help determine the trend of biofilm quantity change in the waterwheel-rotating cage module during an actual sewage operation.

#### 2.3.3. The SOUR Activity of Microorganism Measurements

The specific oxygen utilization rate (SOUR) reflected the dissolved oxygen (DO) consumed by microorganisms per unit weight in unit time and is an important indicator of microbial activity. During tests, a certain amount of biofilm and 150 mL of raw water from the reactor was added to a 250 mL triangular flask, which was quickly sealed with a rubber stopper. Then, it was placed on a magnetic mixer with the rotor speed set at 180 r/min. The temperature was maintained at 25 °C. The DO value was recorded every 3 min for 30 min through an oxygen electrode. According to the Time–DO value curve, the linear slope of the fitted line was the SOUR activity.

#### 2.3.4. Scanning Electron Microscope (SEM)

Carriers were taken out from the reactor for scanning electron microscope (SEM) analysis. The carriers were dipped in 200 mL of raw water from the reactor and sonicated

for 10 min to remove the attached biomass. The removed biofilm samples were washed with phosphate buffer (0.1, M; pH, 7.0) and fixed with 2.5% glutaraldehyde solution for more than 12 h at 4 °C. Then, the sludge samples were washed twice in phosphate buffer and subsequently dehydrated with ethanol solutions graded from 50% to 100% for 20 min each. Samples were dried by critical point drying (liquid CO<sub>2</sub>) before SEM (SU8020, Hitachi Limited, Tokyo, Japan) observations.

### 2.3.5. EPS Extraction and Analysis

Extracellular polymeric substances (EPSs) were extracted using the cation exchange resin (CER) method [23]. The biofilm sludge was collected using centrifugation for 20 min, and CER was added at a dosage of 70 g/g VSS. The intermixture was stirred for 3 h at 200 rpm, at 4 °C, and settled for 3 min to remove the CER. After centrifugation at 9000 × g at 4 °C for 20 min, and then filtration through 0.45 mm acetate cellulose membranes, an EPS solution for analysis was obtained. Polysaccharides were determined using the anthrone method with glucose as the standard [24]. Proteins were determined using the Lowry method with egg albumin as the standard [25]. Both proteins and polysaccharides results were the average value of three parallel samples. To identify the functional groups in the EPSs, the EPS solution samples were injected into a closed liquid tank before Fourier-transform infrared spectroscopy (FTIR) observation. The liquid layer thickness was between 0.01–1 mm.

### 2.3.6. High-Throughput Sequencing

16SrRNA high-throughput sequencing was chosen to characterize the microbial communities in this process. The amplified region of the sludge samples collected from the integrated reactor (including biofilm sludge on carriers in the waterwheel-rotating cage and sludge in the anaerobic pool) was 338F\_806R. The testing process was performed according to the previous report [26]. The bacterial read data were analyzed using USEARCH.

## 3. Results and Discussion

### 3.1. Performance of the WRBC System

#### 3.1.1. The Start-Up

To achieve rapid recovery of nitrifier activity, the reactor was replenished with aeration in the first 3 days after it was started, and the DO in the waterwheel-rotating cage module was maintained above 7.5 mg/L. The purpose was to achieve rapid recovery of nitrifier activity. The rapid growth of nitrifiers and heterotrophic bacteria thickened the biofilm, and thus denitrifiers can obtain favorable growth conditions. It was not necessary to provide supplementary aeration; however, it was used to accelerate the system startup. Afterwards, the aeration device was removed and dissolved oxygen in the liquid phase was recovered to 1.5–2.5 mg/L. Most of the biofilms were attached to the carrier surface and embedded inside. The biofilm thickness on the carrier was between 0–0.1 mm at 2 d and increased to 0.8–1 mm at 10 d (with a thin biofilm on the container wall observed in some areas). At 19 d, the biofilm thickness was between 2.5–3.0 mm. With the increase in time, the color of the biofilm gradually changed from light brown to dark brown. Microscopic observation of the microorganisms in the biofilm sludge at 19 d showed that rotifers, vorticella, and nematodes appeared in the reactor, indicating a complex microbial population and a long food chain. As shown in Figure 1, NH<sub>4</sub><sup>+</sup>-N, TN, and COD removal efficiency reached above 99%, 95%, and 75% at the same time. Thus, the start-up of the reactor was considered to be completed.

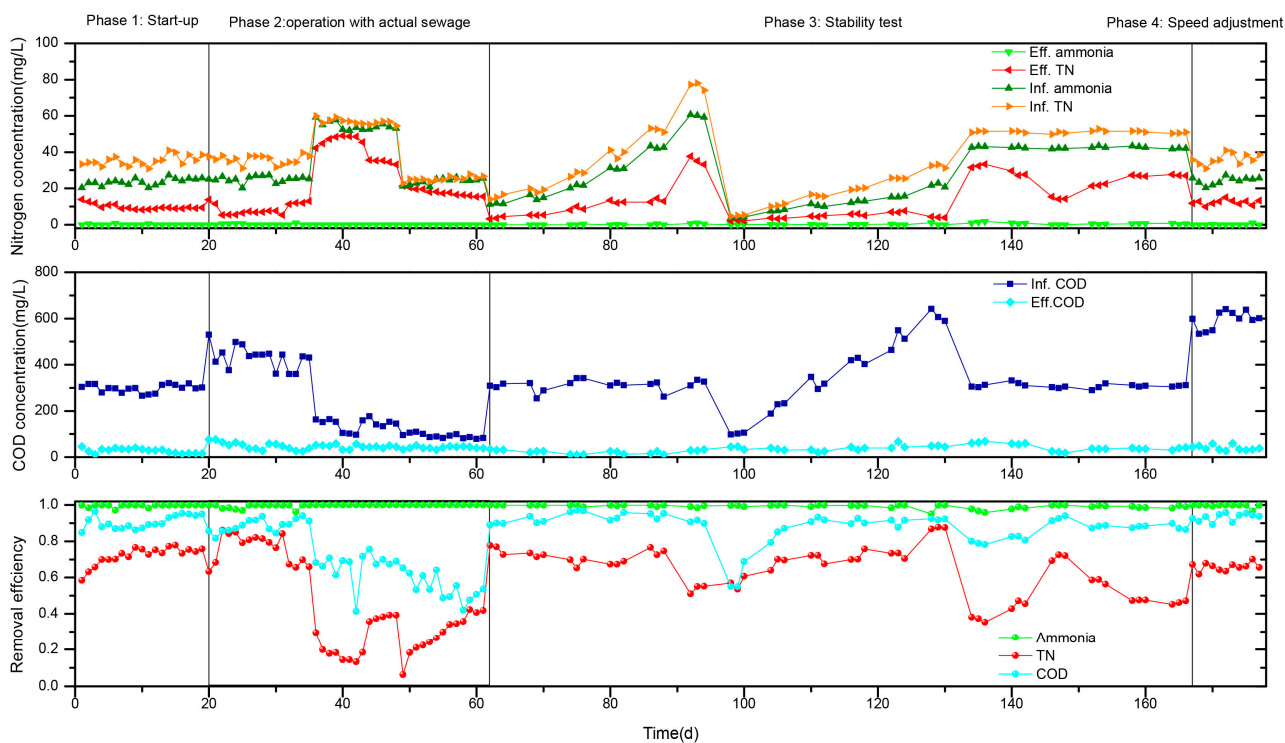


**Figure 1.** Removal performances of the WRBC system.

### 3.1.2. Actual Sewage Treatment Effect

A COD removal efficiency decrease was observed when the WRBC system was fed with actual rural sewage. This demonstrated that the system was still in the adaptation period. A week later, the TN and COD removal efficiency reached above 80% and 90% again. After changing the sampling point of the village wastewater, the COD removal efficiency of the WRBC system decreased from 91% to 68%. This was mainly due to less available carbon sources in the influents. Although the inflow COD concentration fluctuated greatly, the effluent COD concentration was stable and fluctuated between 30–60 mg/L. Taking the time series of the COD removal efficiency of the WRBC system from day 20 to day 61 as the object, the ADF (augmented Dickey–Fuller) test [27] was carried out. Results showed that there was no unit root ( $p$ , 0.003) at this stage, indicating that COD removal of the WRBC system was considered stable with great confidence (>95%). The total biofilm amount was 3115 mg/L at 20 d, and changed to 1918 mg/L at 40 d. At 45 d, the total biofilm amount was recovered to 2091 mg/L. Its change pattern was consistent with the pollutant removal performance.

The WRBC system adapted to the change in  $\text{NH}_4^+\text{-N}$  concentration in the sewage. The  $\text{NH}_4^+\text{-N}$  removal efficiency was stable (above 99%). When dealing with actual sewage from sampling point 1, the effluent TN concentration ranged from 5 to 14 mg/L, and the TN removal efficiency ranged from 65 to 86%. After changing the sampling point of the village wastewater, the TN removal efficiency dropped evidently, mostly because the insufficient influent carbon source affected denitrification. The intake COD/N was less than 3 and the TN removal efficiency was about 40%. Based on this phenomenon, it might not be ideal to build long pipe networks to transfer scattered rural sewage to water treatment plants. First of all, this action was inefficient and not economical. Secondly, the biochemical capacity of sewage at the end of the rural pipe networks was greatly reduced, especially in the rainy season. Better results might be achieved by dispersing sewage treatment facilities as close to residential areas as possible.

### 3.1.3. Stability of the WRBC System

In the system stability tests of nitrogen load impacts, influent nitrogen concentration/37.5 mg/L was set at 40%, 50%, 67%, 100%, 133%, and 200% in order (each for 3 days).

As shown in Figure 2, the average COD removal efficiencies under different N loads were 89.7%, 91.6%, 96.7%, 93.4%, 94.3%, and 90.7% respectively. With the effluent quality under a 100% N load taken as the base, it was found that the COD removal performance had little change. The change rates were  $-3.96\%$ ,  $-1.93\%$ ,  $+3.53\%$ ,  $0$ ,  $+0.96\%$ , and  $-2.89\%$ , respectively, indicating a good COD removal stability of the system. The average TN removal efficiencies were 75.8%, 72.5%, 68.4%, 67.9%, 74.6%, and 53.8%, respectively. The change rates were  $+11.6\%$ ,  $+6.7\%$ ,  $+2.0\%$ ,  $0$ ,  $+9.9\%$ , and  $-20.0\%$ , within the acceptable range. Under the impact of a 200% N load, the TN removal efficiency decreased significantly because the lack of a carbon source limited the denitrification process. In addition, the effluent quality under the impact of a 133% N load was better than that of 100%. The main reason may be that the reactor was operated under a 100% N load for 9 days, and the system's biological community returned to a good growth state for the next impact.

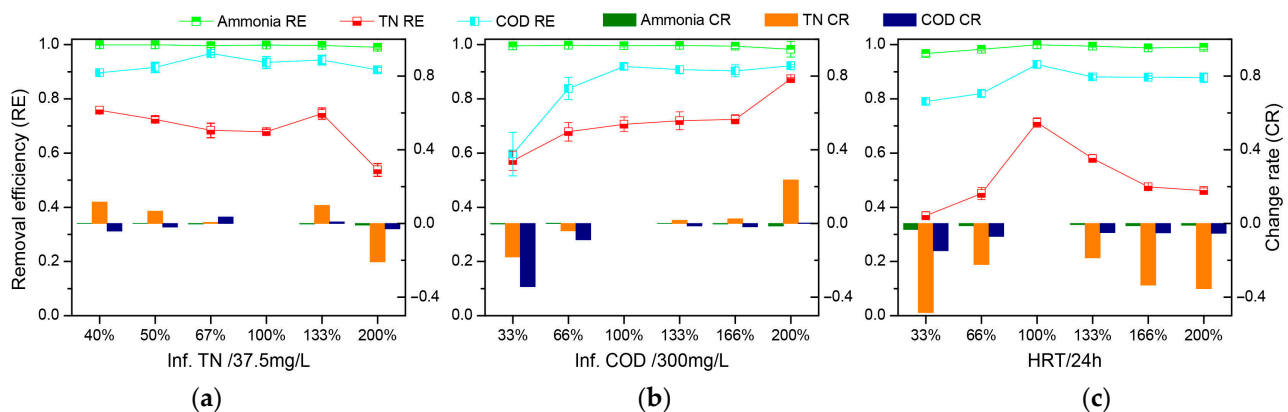


**Figure 2.** Mean value of the removal efficiency of the WRBC system during the stability testing period: (a) N loads impact; (b) COD loads impact; and (c) flow impact.

In the system stability tests under different COD loads (days 98–133), the influent COD concentration/300 mg/L was set at 33%, 66%, 100%, 133%, 166%, and 200% in order. Taking the effluent quality under 100% COD loads as the base, the change rates of the COD removal efficiency under different COD loads were within 8%, except for that under the 33% COD load impact. However, the COD concentration of effluents was lower than 45 mg/L due to the low concentration of influent (100 mg/L), which also met the discharge requirements. The removal efficiency of  $\text{NH}_4^+$ -N in the system was always stable at about 99%. The removal stability of TN was good, and the change rate was within 20%. The augment of COD concentration in influents increased the available substrate of microorganisms, enhancing the activity of denitrifying bacteria and the TN removal capacity.

In the system stability tests under flow impact loads (days 134–166), HRT/24 h was set at 33%, 66%, 100%, 133%, 166%, and 200% in order. The average COD removal efficiencies were 79.0%, 82.0%, 92.7%, 88.1%, 88.0%, and 87.8% respectively. The average TN removal efficiencies were 36.9%, 45.7%, 71.3%, 58.0%, 47.5%, and 46.1% respectively. The sudden increase or decrease in water volume could significantly affect TN removal. Therefore, it was necessary to build a regulating tank to ensure the stability of the inflow when the WRBC system was applied in practical engineering. Based on the formula of the denitrification process, the limited influent COD/N and limited DO concentration implied that a small quantity of nitrogen might be removed through a simultaneous partial nitrification and denitrification process.

In phase 4, the rotation speed was raised to 8 r/min to increase the self-reflux rate. The results showed that the TN removal was not further improved. The SEM results might explain the reason.

### 3.2. Biofilm Morphology and EPS Composition

#### 3.2.1. Surface Morphology of Biofilm

SEM analysis to detect the biofilm surface morphology showed that the packing surface was very smooth at day 0 (as shown in Figure 3). At day 10, a large number of microorganisms was observed to appear on the surface of the filler, with bacillus species and coccus as the main dominant microorganisms. Filamentous bacteria surrounded the bacteria, making microorganisms intertwine to form zoogloea. The microbial biomass was more abundant at day 20, still mainly consisting of bacillus and coccus. EPSs were observed to exist in large quantities, which were secreted by mature biofilms. EPSs contributed to the formation of a cohesive three-dimensional structure and played a role in immobilizing microbial cells. The internal and surface gaps of the intercellular biofilms were the discharge channels of gas produced by the internal denitrifying bacteria. After the introduction of actual sewage, the biofilm collected at day 60 consisted of more compact clusters and the biofilm surface was more uneven than before. At 175 d, the rotational speed of the waterwheel-rotating cage was already set at 8 r/min for several days. Some of the bacteria on the surface were disrupted by the water flow shear force, which explained the lower activity of biofilm sludge. The SOUR activity of microorganisms in the biofilm sludge was 0.22 mgO<sub>2</sub>, 0.18 mgO<sub>2</sub>, and 0.16 mgO<sub>2</sub>/gMLVSS·min at 20 d, 60 d, and 170 d, which was partly related to the state of the biofilm.

#### 3.2.2. Composition of EPSs

Polysaccharide and protein contents of inoculated sludge (day 0), and biofilm sludge collected after the system was started up (day 20) and after treating actual sewage (day 40), were analyzed. As shown in Figure 4a, polysaccharide contents were 27.6 mg, 48.2 mg, and 37.2 mg/g.VSS, which acted as binders inside the biofilm. The decrease in polysaccharide contents over time was associated with the change in the total biofilm amount. Proteins were often present on the biofilm surfaces in the form of extracellular enzymes. Due to the decrease in N and COD concentrations in the incoming water, the amount of protein synthesis was affected and the protein contents changed from 40.7 mg to 36.8 mg/g.VSS.

To further explore the situation of the active functional group, inoculated sludge and biofilm sludge were analyzed by FTIR technology. As shown in Figure 4b, the infrared patterns of EPSs in biofilm sludge at different stages were similar, indicating no significant change in the functional groups in the biofilms over time. The range of the wavenumber at 4000–1330 cm<sup>-1</sup> belonged to the characteristic frequency range of the infrared spectrogram. The absorption peak in this area was basically generated by the stretching vibration of the active group, which was used in the identification of functional groups. Significant energy absorption occurred in the range of 2800–3900 cm<sup>-1</sup>, probably caused by the stretching vibration of C-H, =CH<sub>2</sub>, ≡CH, -OH, and -NH<sub>2</sub> groups. The peak spectrum was wide because there were various functional groups of polysaccharides and proteins in the system, which interlapped and influenced each other. Compared with the inoculated sludge, the peak strength of 3200–3500 cm<sup>-1</sup> was significantly enhanced, most likely due to the increase in the -NH<sub>2</sub> group content. This was related to the increase in the protein content in the system, such as enzymes. The spectrum showed that energy absorption occurred near 1645 cm<sup>-1</sup>, which was mainly caused by the stretching vibration of the C=C group, together with the deformation vibration of crystal water (-OH) and the N-H group. The intensity of the vibration absorption peak was related to the polarity of the bond, indicating that the C=C group had a large influence. According to the spectrum, energy absorption happened near 1410 cm<sup>-1</sup>, which was mainly caused by the stretching vibration of COO-, together with the deformation vibration of alkyl and the bending vibration of -OH, proving that there might be glucose. In addition, SH, C≡N, and -NO<sub>2</sub> did not exist in the system.

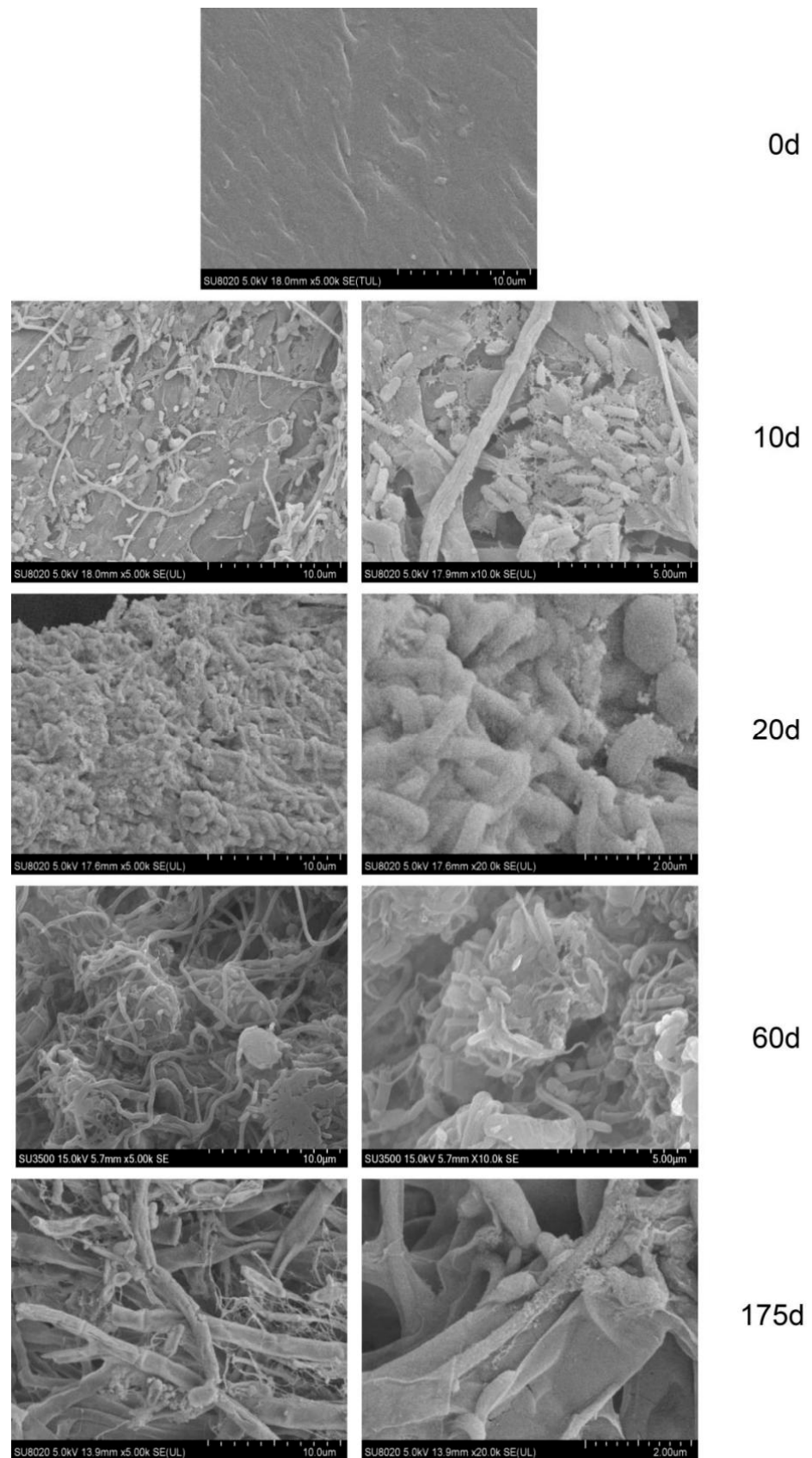
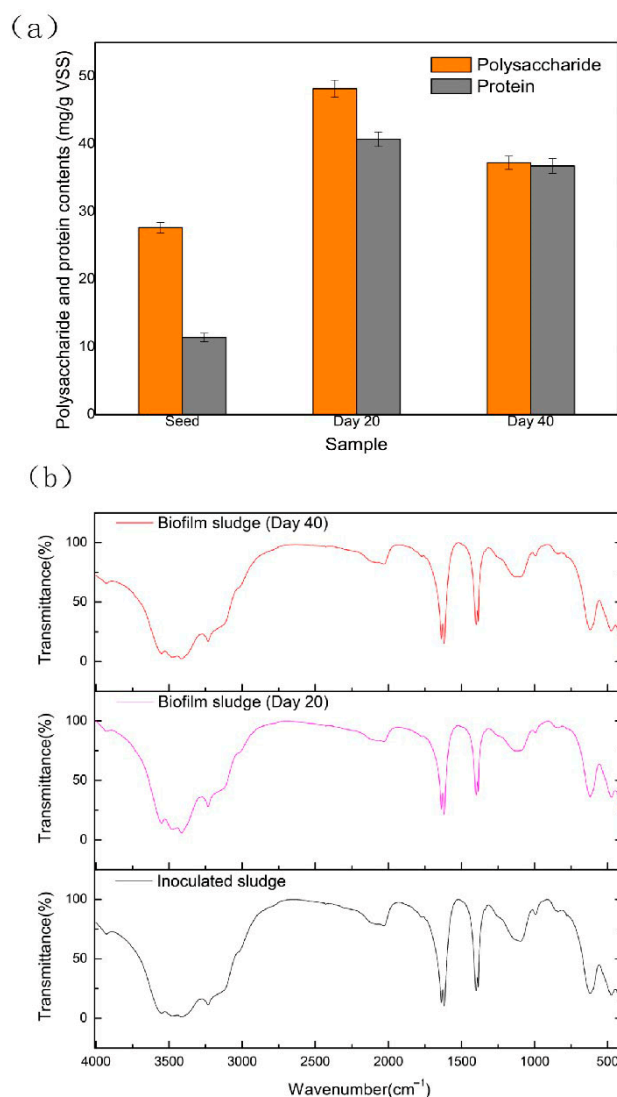


Figure 3. Scanning electron micrographs of biofilm sludge in the WRBC system.



**Figure 4.** EPS comparison of inoculated sludge and biofilm sludge in the WRBC system: (a) polysaccharide and protein contents in EPSs; (b) infrared spectra of EPSs.

### 3.3. Microbial Community

#### 3.3.1. Bacterial Diversity

High-throughput sequencing of 16SrRNA was conducted to characterize the microbial population structure in the WRBC system. Sludge samples O1–O3 were collected from carriers in the waterwheel-rotating cage on day 20, day 60, and day 160, respectively, while A1–A3 were collected from the anaerobic pool. The sludge sample seed was the inoculated sludge. Based on 97% similarity, sequences were assigned into 6524 ASVs (amplicon sequence variant), 1745 species, 930 genera, 504 families, 125 orders, 119 classes, and 41 phyla. Due to the use of real-time actual sewage, species richness was significantly higher than that in other studies. The bacterial diversity of ASV based on analyses of  $\alpha$ -diversity indices and rarefaction curves are shown in Figure 5. The ACE estimator and the Shannon diversity index showed that the species richness of biofilm sludge from the waterwheel-rotating cage was lower than that of the anaerobic pool. The microbial diversity obviously increased after the treatment of the actual sewage, mainly because new organisms were introduced into the system. During phase 3 with artificial influents, the microbial diversity level returned to near that of 20 d. The rarefaction curve revealed that the produced data were enough to cover all species.



### 3.3.2. Microbial Community Structure

The main phyla in the WRBC system were *Proteobacteria*, *Chloroflexi*, *Actinobacteriota*, *Bacteroidota*, and *Acidobacteriota*. These phyla were commonly found in RBC systems in previous studies. The proportion of the sequences assigned into *Proteobacteria* accounted for 53.9%, 48.9%, and 51.9% in biofilm sludge from the waterwheel-rotating cage on day 20, day 60, and day 160, respectively; this was higher than that in the anaerobic pool in the same period. Most denitrifiers, some members of nitrogen-fixation bacteria, and nitrifying bacteria fell into the category of *Proteobacteria*. The second dominant phylum was *Chloroflexi*, showing more abundance in the anaerobic pool. Some members of *Chloroflexi* acted as the skeletons of sludge flocs and could be scavengers of organic matter derived from other bacterial cells [28]. The role of *Chloroflexi* in the anaerobic process could be hydrolytic fermentation. *Actinobacteriota* gradually gained a more dominant growth position over time, consistent with SEM observations, while the relative proportion of *Bacteroidota* decreased. The proportion of bacteria belonging to *Acidobacteriota* increased slightly in the anaerobic pool, and decreased in the waterwheel-rotating cage with operation time. Some acidobacteria had the ability to use nitrite as an N source, degrade gellan gum, and produce exopolysaccharides.

After the treatment of actual sewage, the abundance of some bacteria increased, including *norank\_f\_JG30-KF-CM45*, *Nitrospira*, *Rhodobacter*, etc. *Nitrospira* was the dominant nitrifying bacteria present in the WRBC system. *Rhodobacter* can use a variety of organic compounds as carbon sources and electron donors for photoheterotrophic growth under anaerobic conditions [26]. It can fix nitrogen and is the first free-living bacteria to be known to utilize the regulatory methods associated with quorum sensing. Bacteria with quorum-sensing systems possessed certain signaling compounds which allow the organism to communicate and coordinate with similar bacteria. *Pedomicrobium* was also introduced with the actual sewage treatment, which can remove manganese to reduce the murkiness of the water. Its presence was associated with the abundance of manganese deposits in the soil and groundwater in the sampled villages.

Bacteria with reduced abundance after treatment of actual sewage included *Ahniella*, *Phreatobacter*, *norank\_f\_Caldilineaceae*, etc. *Phreatobacter* lived in a low-nutrient environment and had strong utilization of the matrix. In addition, *Thiothrix* existed in this system, which can grow with sulfide as its only energy source. It can easily reproduce under low dissolved oxygen and is considered to be one of the main causes of activated sludge expansion. The phylogenetic tree showed the relatedness of bacteria with an abundance ratio of the top 30 in biofilm sludge from the waterwheel-rotating cage at the genus level (see Figure 5e). According to the phylogenetic tree, one could guess that the characteristics of some bacteria not classified or ranked could be inferred. *norank\_Saprospiraceae* had a close relationship with *Terrimonas*, which might also use glucose and lactose. *SWB02* and *unclassified\_f\_Hyphomonadaceae* formed a very close relationship with *Hyphomicrobium*, and could probably perform denitrification.

### 3.3.3. Functional Bacterium

Based on sequencing data, bacteria with nitrification and denitrification functions were detected and graphed for analysis (as shown in Figure 6). *Ellin6067* (belonging to *Nitrosomonadaceae*) and *Nitrospira* with the function of autotrophic nitrification were discovered to increase obviously on day 60 in the waterwheel-rotating cage. The possible reason was that the influent COD of days 40–60 was low, making the metabolic activity of heterotrophic bacteria lower and the DO in the liquid higher. It created a suitable environment for nitrifying bacteria enrichment. *Nitrospira* existed in the anaerobic pool, which was influenced by the sampling location. The self-reflux liquid returned to the anaerobic pool through a weir (see graphic abstract) and biofilms hanging on the reactor wall near its inlet grew thicker. The biofilm sludge sampling point was set here. On the one hand, the DO value of the self-reflux liquid was high, creating an environment conducive to *Nitrospira*

growth. On the other hand, microorganisms from the waterwheel-rotating cage returned to the anaerobic pool with the water flow.

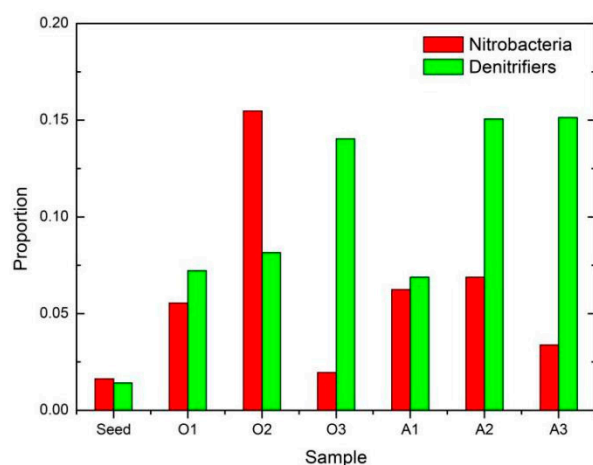


**Figure 6.** Distribution of nitrobacteria and denitrifiers.

As recorded in the statistics, denitrifiers appeared in the WRBC system included *Acidovorax*, *Arenimonas*, *Azospira*, *Bacillus*, *Comamonas*, *Delftia*, *Devosia*, *Flavobacterium*, *Hydrogenophaga*, *Hyphomicrobium*, *Paracoccus*, *Pseudomonas*, *Pseudoxanthomona*, and *Thauera*. *Hyphomicrobium* could realize simultaneous and intermittent nitrification and denitrification. The last three were reported to be able to carry out heterotrophic nitrification–aerobic denitrification of bacteria. In the anaerobic pool, the population of denitrifying bacteria was more than that in the waterwheel-rotating cage. With the operation time, the abundance of denitrifying bacteria in the biofilm sludge of the waterwheel-rotating cage increased significantly. On day 160, the proportion of denitrifiers accounted for more than 14%, indicating that biofilm formed stable external aerobic and internal anaerobic states.

#### 4. Conclusions

A novel WRBC system was developed to treat rural sewage with high-shock load resistance.  $\text{NH}_4^+\text{-N}$ , TN, and COD removal efficiency reached above 99%, 95%, and 75% with artificial simulated sewage after startup. When the COD concentration of actual sewage fluctuated between 79–530 mg/L, the COD removal efficiency was 41.3–94.5% and the effluent COD concentration was stable and fluctuated between 30–60 mg/L. The  $\text{NH}_4^+\text{-N}$  removal efficiency reached 100% with actual sewage. The TN removal efficiency changed between 14.3–86.2%, which was greatly affected by the water intake. However, the effluent TN concentration ranged from 5 to 14 mg/L, which meets the emission requirements. It maintained an absolute effluent stability when the change rates of influent loads (N/COD) varied from –60% to 100%. SEM results showed that the biofilm formed more uneven compact clusters after the treatment of actual sewage. Some of the bacteria on the surface were disrupted by the water flow shear force if the rotational speed of the waterwheel-rotating cage was enhanced to 8 r/min. FTIR spectra results showed no significant change in the functional groups in the biofilms over time. However, the  $\text{-NH}_2$  group content increased compared with the inoculated sludge due to the increase in protein content in the system, such as enzymes. Based on 16SrRNA high-throughput sequencing techniques, the bacterial diversity and microbial community structure of the WRBC system over time were revealed.

**Author Contributions:** J.H.: conceptualization, investigation, methodology, data curation, funding acquisition, writing—original draft; X.W.: conceptualization, investigation, methodology, data curation, funding acquisition, writing—original draft; Q.T.: investigation, methodology, data curation; D.L.: resources, supervision; S.C.: software, validation. All authors have read and agreed to the published version of the manuscript.

**Funding:** This work was supported by the Natural Science Foundation Project of Chongqing (grant numbers cstc2018jszx-zdyfxmX0001 and cstc2019jcyj-msxmX0562), the Science and Technology Research Program of Chongqing Municipal Education Commission (grant number KJQN202001515), and the Provincial and Ministerial Co-constructive of Collaborative Innovation Center for MSW Comprehensive Utilization (grant numbers shljzyh2021-09 and shljzyh2021-22).

**Data Availability Statement:** Not applicable.

**Conflicts of Interest:** The authors declare that they have no known competing financial interests or personal relationships that could have appeared to influence the work reported in this paper.

## References

1. Li, X.; Yang, L.; Xu, K.; Bei, K.; Zheng, X.; Lu, S.; An, N.; Zhao, J.; Jin, Z. Application of constructed wetlands in treating rural sewage from source separation with high-influent nitrogen load: A review. *World J. Microbiol. Biotechnol.* **2021**, *37*, 138. [[CrossRef](#)] [[PubMed](#)]
2. Jin, Z.; Zheng, Y.; Li, X.; Dai, C.; Xu, K.; Bei, K.; Zheng, X.; Zhao, M. Combined process of bio-contact oxidation-constructed wetland for blackwater treatment. *Bioresour. Technol.* **2020**, *316*, 123891. [[CrossRef](#)] [[PubMed](#)]
3. Wu, Y.; Wan, A.; Zhao, B.; Xue, S.; Xu, A. Single-stage MBBR using novel carriers to remove nitrogen in rural domestic sewage: The effect of carrier structure on biofilm morphology and SND. *J. Environ. Chem. Eng.* **2022**, *10*, 108267. [[CrossRef](#)]
4. Li, W.; Zheng, T.; Ma, Y.; Liu, J. Fungi characteristics of biofilms from sewage and greywater in small diameter gravity sewers. *Environ. Sci. Water Res. Technol.* **2020**, *6*, 532–539. [[CrossRef](#)]
5. Piasecki, A. Water and sewage management issues in rural poland. *Water* **2019**, *11*, 625. [[CrossRef](#)]
6. Sadeghfam, S.; Abadi, B. Decision-making process of partnership in establishing and managing of rural wastewater treatment plants: Using intentional and geographical-spatial location data. *Water Res.* **2021**, *197*, 117096. [[CrossRef](#)]
7. Ding, R.; Li, Y.; Yu, X.; Peng, Y.; Zhang, Z.; Wei, L. Characteristics of rural agritainment sewage in Sichuan, China. *Water Sci. Technol.* **2019**, *79*, 1695–1704. [[CrossRef](#)]
8. Cao, X.; Jiang, L.; Zheng, H.; Liao, Y.; Zhang, Q.; Shen, Q.; Mao, Y.; Ji, F.; Shi, D. Constructed wetlands for rural domestic wastewater treatment: A coupling of tidal strategy, in-situ bio-regeneration of zeolite and Fe(II)-oxygen denitrification. *Bioresour. Technol.* **2022**, *344*, 126185. [[CrossRef](#)]
9. Chaves-Barquero, L.G.; Luong, K.H.; Rudy, M.D.; Frank, R.A.; Hanson, M.L.; Wong, C.S. Attenuation of pharmaceuticals, nutrients and toxicity in a rural sewage lagoon system integrated with a subsurface filtration technology. *Chemosphere* **2018**, *209*, 767–775. [[CrossRef](#)]
10. Zheng, H.; Jiang, L.; Cao, X.; Liao, Y.; Mao, Y.; Ji, F. A combined deodorization reflux system and tidal flow constructed wetland for sewage treatment performance. *J. Environ. Chem. Eng.* **2021**, *10*, 106953. [[CrossRef](#)]
11. Jia, L.; Sun, H.; Zhou, Q.; Zhao, L.; Wu, W. Pilot-scale two-stage constructed wetlands based on novel solid carbon for rural wastewater treatment in southern china: Enhanced nitrogen removal and mechanism. *J. Environ. Manag.* **2021**, *292*, 112750. [[CrossRef](#)] [[PubMed](#)]
12. Fan, Z.; Liang, Z.; Luo, A.; Wang, Y.; Ma, Y.; Zhao, Y.; Lou, X.; Jia, R.; Zhang, Y.; Ping, S. Effect on simultaneous removal of ammonia, nitrate, and phosphorus via advanced stacked assembly biological filter for rural domestic sewage treatment. *Biodegradation* **2021**, *32*, 403–418. [[CrossRef](#)] [[PubMed](#)]
13. Han, Y.; Ma, J.; Xiao, B.; Huo, X.; Guo, X. New integrated self-refluxing rotating biological contactor for rural sewage treatment. *J. Clean. Prod.* **2019**, *217*, 324–334. [[CrossRef](#)]
14. Ding, A.; Wang, J.; Lin, D.; Tang, X.; Cheng, X.; Li, G.; Ren, N.; Liang, H. In situ coagulation versus pre-coagulation for gravity-driven membrane bioreactor during decentralized sewage treatment: Permeability stabilization, fouling layer formation and biological activity. *Water Res.* **2017**, *126*, 197–207. [[CrossRef](#)] [[PubMed](#)]
15. Zhao, Y.; Wang, H.; Dong, W.; Chang, Y.; Yan, G.; Chu, Z.; Ling, Y.; Wang, Z.; Fan, T.; Li, C. Nitrogen removal and microbial community for the treatment of rural domestic sewage with low C/N ratio by A/O biofilter with *Arundo donax* as carbon source and filter media. *J. Water Process Eng.* **2020**, *37*, 101509. [[CrossRef](#)]
16. Chen, G.; Huang, J.; Fang, Y.; Zhao, Y.; Tian, X.; Jin, Y.; Zhao, H. Microbial community succession and pollutants removal of a novel carriers enhanced duckweed treatment system for rural wastewater in Dianchi lake basin. *Bioresour. Technol.* **2019**, *276*, 8–17. [[CrossRef](#)] [[PubMed](#)]
17. Li, Y.; Chen, W.; Zheng, X.; Liu, Q.; Xiang, W.; Qu, J.; Yang, C. Microbial community structure analysis in a hybrid membrane bioreactor via high-throughput sequencing. *Chemosphere* **2021**, *282*, 130989. [[CrossRef](#)]
18. Wang, L.; Guo, F.; Zheng, Z.; Luo, X.; Zhang, J. Enhancement of rural domestic sewage treatment performance, and assessment of microbial community diversity and structure using tower vermifiltration. *Bioresour. Technol.* **2011**, *102*, 9462–9470. [[CrossRef](#)]
19. Barwal, A.; Chaudhary, R. To study the performance of biocarriers in moving bed biofilm reactor (MBBR) technology and kinetics of biofilm for retrofitting the existing aerobic treatment systems: A review. *Rev. Environ. Sci. Bio/Technol.* **2014**, *13*, 285–299. [[CrossRef](#)]
20. Waqas, S.; Bilal, M.R. A review on rotating biological contactors. *Indones. J. Sci. Technol.* **2019**, *4*, 241–256. [[CrossRef](#)]

21. APHA. *Standard Methods for the Examination of Water and Wastewater*; American Public Health Association (APHA): Washington, DC, USA, 2012.
22. Glaskova, T.; Zarrelli, M.; Borisova, A.; Timchenko, K.; Aniskevich, A.; Giordano, M. Method of quantitative analysis of filler dispersion in composite systems with spherical inclusions. *Compos. Sci. Technol.* **2011**, *71*, 1543–1549. [[CrossRef](#)]
23. Frølund, B.; Palmgren, R.; Keiding, K.; Nielsen, P.H. Extraction of extracellular polymers from activated sludge using a cation exchange resin. *Water Res.* **1996**, *30*, 1749–1758. [[CrossRef](#)]
24. Dogan, N.M.; Doganli, G.A.; Dogan, G.; Bozkaya, O. Characterization of extracellular polysaccharides (EPS) produced by thermal Bacillus and determination of environmental conditions affecting exopolysaccharide production. *Int. J. Environ. Res.* **2015**, *9*, 1107–1116.
25. Sheng, G.P.; Yu, H.Q. Characterization of extracellular polymeric substances of aerobic and anaerobic sludge using three-dimensional excitation and emission matrix fluorescence spectroscopy. *Water Res.* **2006**, *40*, 1233–1239. [[CrossRef](#)]
26. Wen, X.; Huang, J.; Zeng, G.; Liu, D.; Chen, S. Microbial activity along the depth of biofilm in simultaneous partial nitrification, anammox and denitrification (SNAD) system. *Environ. Technol.* **2022**, 1–8. [[CrossRef](#)]
27. Matsumoto, C.; Yanagihara, H.; Wakaki, H. Improvement of the quality of the chi-square approximation for the ADF test on a covariance matrix with a linear structure. *J. Stat. Plan. Inference* **2011**, *141*, 1535–1542. [[CrossRef](#)]
28. Wen, X.; Gong, B.; Zhou, J.; He, Q.; Qing, X. Efficient simultaneous partial nitrification, anammox and denitrification (SNAD) system equipped with a real-time dissolved oxygen (DO) intelligent control system and microbial community shifts of different substrate concentrations. *Water Res.* **2017**, *119*, 201–211. [[CrossRef](#)]

**Disclaimer/Publisher’s Note:** The statements, opinions and data contained in all publications are solely those of the individual author(s) and contributor(s) and not of MDPI and/or the editor(s). MDPI and/or the editor(s) disclaim responsibility for any injury to people or property resulting from any ideas, methods, instructions or products referred to in the content.